Identification of Regulatory Factors Promoting Embryogenic Callus Formation in Barley Through Transcriptome Analysis

Jingqi Suo
Zhejiang University
Chenlu Zhou
Zhejiang University
Zhanghui Zeng
Zhejiang University
Xipu Li
Zhejiang University
Hongwu Bian
Zhejiang University
Junhui Wang
Zhejiang University
Muyuan Zhu
Zhejiang University
Ning Han (ninghan@zju.edu.cn)
Zhejiang University

Research Article

Keywords: Barley (Hordeum vulgare), callus induction, auxin response, plant regeneration

Posted Date: December 9th, 2020

DOI: https://doi.org/10.21203/rs.3.rs-116630/v1

Version of Record: A version of this preprint was published on March 19th, 2021. See the published version at https://doi.org/10.1186/s12870-021-02922-w.

Abstract

Background: Barley is known to be recalcitrant to tissue culture, which hinders genetic transformation and its biotechnological application. To date, the ideal explant for transformation is still limited to immature embryos; however, the mechanism underlying embryonic callus formation remains elusive.

Results: The aim of this study was to uncover the differential transcription regulation pathways between immature embryo (IME)- and mature embryo (ME)-derived callus formation through transcriptome sequencing. We showed that incubation of embryos on auxin-rich medium caused dramatic changes in gene expression profiles within 48 h. A total of 9330 and 11318 differentially expressed genes (DEGs) were found in the IME and ME systems, respectively. Protein phosphorylation, regulation of transcription, and oxidative-reduction process were the most common gene ontology categories of DEGs specific to the IME system. Twenty-three *IAA*, 14 *ARF*, 8 *SAUR*, 3 *YUC*, and 4 *PIN* genes were found to be differentially expressed during callus formation. The effect of callus-inducing medium (CIM) on *IAA* genes was broader in the IME system than in the IM system, indicating that auxin response and transport cooperate in regulating cell reprogramming during callus formation. *BBM*, *LEC1* and *PLT2* exhibited a significant increase in expression level during IME system but were not activated in the ME system, *WUS* showed a more substantial growth trend in the IME system than in the ME system, suggesting that these embryonic, shoot, and root meristems genes play crucial roles in determining the acquisition of competency. In addition, epigenetic regulators—including *SUVH3A*, *SUVH2A*, *HDA19B/703*—exhibited differential expression patterns between the two induction systems, indicating that epigenetic reprogramming might contribute to gene expression activation/suppression in this process. Furthermore, we examined the effect of ectopic expression of *HvBBM* and *HvWUS* on *Agrobacterium*-mediated barley transformation. The transformation efficiency was increased by three times in the group expressing the *PLTPpro:HvBBM* + *Axig1pro:HvWUS* construct, compared to that in the control (empty vector), which was due to an enhancement of plant regeneration capacity.

Conclusions: We identified some regulatory factors that might contribute to the differential responses of the two explants to callus induction and provide a promising strategy to improve transformation efficiency in barley.

Background

Genetic transformation has become an essential tool for functional genome research as well as a useful technique for crop breeding. A routinely used protocol for transformation of monocot species depends on *in vitro* tissue culture. However, many crop cultivars seem to be recalcitrant to regeneration, which is a major bottleneck in plant transformation. Thus, elucidation of the molecular basis of plant regeneration is of great importance for the improvement of plant biotechnology.

A typical *Agrobacterium*-mediated transformation often starts with the induction of pluripotent cells (termed “callus”) from explants cultivated on an auxin-rich CIM. Recent studies have demonstrated that CIM-induced callus formation proceeds via a root meristem-associated pathway [1], displaying an organized spatial expression of root meristem regulator genes such as WUSCHEL-RELATED HOMEOBOX5 (*WOX5*) and SHORT ROOT (*SHR*) [1, 2]. As occurs in lateral root development, auxin leads to the degradation of INDOLEACETIC ACID 14 (IAA14) and subsequent activation of AUXIN RESPONSE FACTOR7 (ARF7) and ARF19 [3]; AFR7 and ARF19 then directly enhance the expression of LATERAL ORGAN BOUNDARIES DOMAIN (LBD) proteins, such as LBD16, LBD17, LBD18, and LBD29 [4, 5]. LBD proteins, in turn, activate the expression of a suite of genes that promote cell proliferation and modify cell wall properties [6-8]. Furthermore, auxin also promotes cellular pluripotency acquisition via two different pathways, one mediated by WOX11 and LBD16 and the other involving CUP-SHAPED COTYLEDON2 (CUC2) and PLETHORA proteins (PLTs) [9, 10]. Since most researchers have used *Arabidopsis* for this procedure, it remains unclear whether different species adopt a

common mechanism for callus initiation. Our previous work demonstrated that callus induction from root explants employs different strategies in rice and *Arabidopsis* [11]. However, it is still unknown whether the same pathway is involved when an embryo is used as the explant.

Barley (*Hordeum vulgare* L.) is the fourth most abundant cereal crop globally and is widely grown as animal feed and for making malt and brewing wine. The first report of successful *Agrobacterium*-mediated transformation in barley used immature embryos as the explant [12]. Although alternative target tissues have been examined for use in barley transformation systems, immature embryos remain the best choice for high transformation efficiencies [13-16]. Moreover, barley transformation is highly genotype dependent. The most responsive genotype is the spring cultivar Golden Promise, and only a few barley varieties have been successfully transformed to date [17]. The genes underlying transformability in Golden Promise have been investigated through genetic mapping [18]. Three transformation-amenability loci in Golden Promise (*TFA1*, *TFA2*, *TFA3*) and one locus in mutant 1460 (*TRA1*) were found to be responsible for *Agrobacterium*-mediated transformation in barley [19, 20]. However, the key factors determining explant choice and transformation efficiency remain elusive.

The aim of this study was to provide new insights into the differential transcription regulation pathways between immature embryo- and mature embryo-derived callus formation through transcriptome sequencing. We outlined a framework of early molecular events behind auxin-induced callus formation in barley, suggesting strategies to enrich the selection range of explants and improve transformation efficiency in barley.

Results

Morphologies of calli formed from mature and immature barley embryos

Because callus induction and transformation efficiency in barley is genotype-dependent, the model barley variety Golden Promise, which has high callus formation capacity, was selected to investigate the mechanism of callus formation in this study. Immature embryos—approximately 14 days post-anthesis (DPA)—and mature embryos, with the embryonic axis removed, were used as explants for callus induction on the same CIM containing 2.5 mg/L dicamba (a synthetic auxin). After 24 h of incubation in CIM, smooth and watery calli, with some degree of normal regeneration (visible shoots), could be seen on the mature seed scutellum. In the IME-induction system, yellow friable callus had emerged from the scutellum's peripheral region after 48 h in the CIM medium (Figure 1a). Almost all immature embryos had generated embryogenic calli and maintained a faster proliferation rate after seven days of cultivation (Figure 1b). After four weeks of cultivation, almost all immature embryos—but only a few mature ones—had developed calli; the few calli formed from mature embryos were watery as compared to the dense and granular calli formed from immature embryos (Figure 1c).

Global analysis of DEGs expressed in calli derived from mature and immature embryos

To obtain an overview of the mRNA expression profile during callus formation on CIM, we constructed cDNA libraries using five samples, each with three biological replicates. Three of the samples were isolated from immature embryo (IME)-derived calli at various time points—IME_0h, IME_24h, and IME_48h. The other two samples were taken from mature embryo (ME)-derived calli at different time points—ME_0h and ME_24h (Figure 1a). Absolute quantitative transcriptome sequencing was then performed using mainstream Unique Molecular Identifier (UMI) labeling technology; through UMI labeling of each sequence, the interference of PCR amplification preference on quantification was eliminated so that the expression abundance of transcripts in the sample could be truly reflected. Raw data totaling 114 Gb was obtained, which contained 759 million paired-end reads. After removing adaptor sequences and low-quality reads, approximately 740 million clean reads remained. Over 99.92% and 97.40% of the clean reads had

quality scores of Q20 and Q30, respectively (Additional file 1: Table S1). More than 90.82% of the paired-end reads were mapped to the barley reference genome, with an average of 69.15% for unigenes (Table 1).

To determine whether this gene expression profile correlated with different stages, read numbers were first normalized to the RPKM value. They were then subjected to the usual correlation coefficient (R^2) and hierarchical clustering analysis. The three biological replicates of all samples showed consistent determinations of transcript abundance with a coefficient (R^2) greater than 0.87, indicating good repeatability of the sequencing data (Additional file 1: Figure S1). Further analyses showed that 125,095 transcripts (74.98%) were between 1000 and 5000 bp in length, and 8021 genes (55.21%) were between 1000 and 5000 bp in length (Additional file 1: Table S2).

The criterion ($|\log_2 \text{fold change}| \geq 1$ and $\text{pvalue} \leq 0.05$) was used for screening differentially expressed genes (DEGs). The DEGs revealed in this study were divided into six groups by pairwise comparison. The group with the largest number of DEGs was the ME_0h vs. IME_0h group, with 5396 upregulated genes and 5913 downregulated genes. For both explants, significant gene expression changes were observed during callus formation (Figure 2a). A venn diagram showed that 859 DEGs were detected in all four comparison groups (IME_0h vs. 48h, ME_0h vs. 24h, IME_0h vs. ME_0h, IME_48h vs. ME_24h). Besides 5450 DEGs, which overlapped in two of the comparison groups (IME_0h vs. 48h, ME_0h vs. 24h), 3880 and 5868 DEGs were identified specifically in immature and mature embryos-based induction systems, respectively. A total of 1480 genes were specifically differentially expressed in the initial phase of mature and immature embryos before induction (IME_0h vs. ME_0h) (Figure 2b).

Gene ontology (GO) analysis showed that protein phosphorylation, regulation of transcription, oxidative-reduction process, membrane, and protein, ATP, and nucleotide binding were the most common GO categories of DEGs specific to the IME system (Figure 2c, Additional file 1: Figure S2). Amino acid metabolism, carbohydrate metabolism, lipid metabolism, and biosynthesis of other secondary metabolites were the most enriched pathways associated with IME-specific DEGs (Figure 2d, Additional file 1: Figure S3).

In addition, we separately analyzed the upregulated and downregulated DEGs of the IME_0h vs. 48h and ME_0h vs. 24h groups. The Venn diagram analysis divided the DEGs into six parts. Only 2962 genes were upregulated during immature-embryo callus induction. The expression of 1637 genes was downregulated during immature-embryo callus induction. The genes of the six parts were analyzed by GO and KEGG (Additional file 1: Figure S2, Additional file 1: Figure S3).

Differential expression of transcriptional regulators involved in callus induction

Transcription factors (TFs) play critical roles in embryogenic callus formation by regulating cell proliferation and cell fate reprogramming [21, 22]. The plant transcription factor database PlantTFDB (http://planttfdb.cbi.pku.edu.cn) was used to sequence blast and annotate the TFs in barley associated with callus initiation in our dataset.

Since we were interested in identifying TFs determining embryonic callus formation, we further analyzed TF transcripts that were differentially regulated only in the IME group. A set of 226 TF genes, including 150 upregulated genes and 76 downregulated genes, were identified as DEGs, specifically during IME-derived callus induction. These TFs may contribute to the differential response of the two explants to callus induction (Figure 3a). In addition, bHLH, NAC, MYB, B3, and HSF family members were among the differentially expressed transcriptional factors enriched in this group (Figure 3b). Among them, significantly differentially expressed TFs, with a fold change greater than 4.5 ($\text{pvalue} < 0.05$), found explicitly in the IME system are shown in Figure 3c. The transcript levels of *AP2* (HORVU1Hr1G011800), *LBD12* (HORVU5Hr1G047610), *MYBH* (HORVU1Hr1G073300), *NAC1* (HORVU7Hr1G106480), and *ERF3* (HORVU3Hr1G030310)

increased, whereas the levels of *ERF109* (HORVU5Hr1G068450), *B3-like* (HORVU4Hr1G012060), and *WRKY3* (HORVU5Hr1G065420) decreased during callus induction.

Dramatic changes in the expression of TFs occurred in both callus induction systems. Four hundred and thirty transcription factors were identified in the IME_0h vs. IME_48h group and four hundred and seventy-two transcription factors were identified in the ME_0h vs. ME_24h group. Among them, bHLH, NAC, bZIP, MYB_related, and ERF ranked in the top five of the IME_0h vs. IME_48h group (Additional file 1: Figure S4a). In addition, bHLH, NAC, ERF, bZIP, and MYB family members were among the differentially expressed transcriptional factors enriched in the ME_0h vs. ME_24h group (Figure S4b). In the IME_0h vs. IME_48h group, the transcript levels of *HD-ZIP1* (HORVU4Hr1G078410), *PRE5* (HORVU4Hr1G075340), *LBD16* (HORVU0Hr1G017670), WUSHEL (*WUS*, HORVU3Hr1G085050), and *ESE3* (HORVU7Hr1G029870) increased, whereas the levels of *ERF48* (HORVU1Hr1G063100), *SRS-like* (HORVU6Hr1G084070), and *C2H2-like* (HORVU5Hr1G112900) declined during callus induction (Figure S4c). In the ME_0h vs. ME_24h group, the transcript levels of *LBD29* (HORVU4Hr1G080160), *bHLH-like* (HORVU3Hr1G030760), and *NAC071* (HORVU1Hr1G049840) increased, whereas the levels of *SRS-like* (HORVU6Hr1G084070), *bZIP-like* (HORVU4Hr1G021720), and *HSF-like* (HORVU2Hr1G040680) appeared to decrease during callus induction (Figure S4d).

Auxin signaling during CIM-mediated callus formation

Auxin has been reported to play vital roles in promoting cell proliferation and reprogramming during callus formation in tissue culture [23-25]. We examined the transcriptional profile of genes related to auxin response, biosynthesis, and transport. Twenty-three *IAA*, 14 *ARF*, 8 *SAUR*, 3 YUCCA (*YUC*), and 4 PIN-FORMED (*PIN*) genes were found to be differentially expressed during the callus formation process (Figure 4). The effect of CIM on *IAA* genes was broader in the IME system than in the ME system. Twenty-two *IAA* candidate genes exhibited a significant increase in expression level when IME was used as the explant; ten *IAA* genes were found to be upregulated (more than 3 times) in the ME group. Most of the analyzed *ARF* genes showed differential expression patterns between the two groups (Figure 4). Notably, candidate genes *ARF11* (HORVU3Hr1G032230) and *ARF16B* (HORVU4Hr1G035810) exhibited an opposite profile between the two groups, and two putative *ARF6* genes (HORVU2Hr1G121110 and HORVU7Hr1G106280) and a candidate gene encoding auxin transporter *PIN1A* (HORVU7Hr1G038700) were upregulated in the IME group but remained unchanged in the ME group. These data indicate that genes associated with auxin transport and response cooperate in regulating cell reprogramming during auxin-induced callus formation.

Changes in the expression of key developmental genes for embryo, root, and shoot meristems during callus formation

Cells are thought to dedifferentiate and acquire competency when they divide to form the callus [2, 26]. To assess the embryogenic character of the embryo-derived callus, marker genes presenting embryo, root, and shoot meristems were analyzed. Among nine putative embryonic genes, the transcripts of FUSCA3 (*FUS3,* HORVU3Hr1G067350) and ABSCISIC ACID-INSENSITIVE 3A (*ABI3A*, HORVU2Hr1G119600) were higher in the IME system than in the ME system. Notably, BABY BOOM (*BBM*, HORVU3Hr1G089160) and *LEC1* (HORVU6Hr1G072110) displayed a significant increase in expression level during IME-derived callus formation but were not activated in the ME system (Figure 5a). The result of quantitative reverse transcription PCR (qRT-PCR) verification was consistent with that of RNA-Seq (Figure 5b, Figure 5c).

Among the eleven upregulated shoot apical meristem (SAM) genes, two genes were only upregulated in the IME system. In addition, transcription of *CUC2* (HORVU5Hr1G045640) and *FILB* (HORVU6Hr1G060770) was rapidly activated during callus formation under the IME system but was suppressed in the ME system. Remarkably, WUSCHEL (*WUS*, HORVU3Hr1G085050) exhibited more significant growth trends in the IME system than in the ME system. Five

root apical meristem (RAM) genes were upregulated, four of which overlapped in two groups. *PLT2* (HORVU3Hr1G089160) displayed a significant increase in expression level during IME-derived callus formation but was not activated in the ME system. The increase in *SHR* (HORVU2Hr1G035730) and *PLT3* (HORVU2Hr1G036590) transcripts was greater in the IME system than in the ME system; *EIR1/PIN2* (HORVU7Hr1G110470) exhibited the opposite pattern (Figure 5a).

Verification of transcriptional regulators might promote embryonic callus formation and transformation

This study identified one *BBM* gene and one *WUS* gene in barley (Additional file 1: Figure S5)—HORVU2Hr1G087310 (termed as *BBM*) and HORVU3Hr1G085050 (termed as *WUS*). These genes exhibited differential expression patterns between the two systems (Figure 6b); thus, we investigated them further in our study. HvBBM contained two AP2 DNA-binding domains, which were highly consistent with the amino acid sequences of genes in maize, rice, and *Arabidopsis thaliana* (Figure 6a). The barley WUS, an ortholog of *Arabidopsis* stem cell regulator WUS [27, 28], contains a HOX domain, a WUS box, and an EAR motif (Figure 6a). Phylogenetic trees showed that the candidate barley *BBM* was closer to the other two monocot genes, and the candidate barley WUS was closer to the WUS of the dicot *Arabidopsis thaliana* (Additional file 1: Figure S5).

To verify the reliability of the sequencing data, qRT-PCR was performed to detect gene expression levels during the early stage of callus formation. The expression level of *HvBBM* increased gradually when immature embryos were used as explants but was decreased during callus induction when mature embryos were used (Figure 6b). This suggests that the *BBM* gene contributes to the differential response of explants to CIM. As for *WUS*, a greater increase in transcription was observed in the IME system than in the ME system (Figure 6b).

We also analyzed the candidate gene *LEC1*. The protein encoded by LEC1 contained one CCAAT binding factor (CBF), with an amino acid sequence highly conserved among barley and other species such as maize, rice, and *Arabidopsis thaliana* (Additional file 1: Figure S6a). The transcript levels of *LEC1* in the five samples were revealed through qRT-PCR, the results of which were consistent with the RNA-seq data (Additional file 1: Figure S6b). Phylogenetic trees showed that the candidate barley LEC1 was closer to the other two homologs in monocots (Additional file 1: Figure S6c).

Ectopic expression of *HvBBM* and *HvWUS* improved genetic transformation efficiency

Overexpression of maize (*Zea mays*) *BBM* and maize *WUS2* genes stimulated transformation in numerous previously non-transformable inbred maize lines, immature sorghum embryos, sugarcane callus, and indica rice callus [29, 30]. In this study, the expression patterns of *BBM* and *WUS* were found to vary between IME- and ME-derived callus induction (Figure 6b). To further investigate the effect of *BBM* and *WUS* ectopic expression on callus formation and transformation efficiency in barley, two constructs were designed, each of which contained two expression cassettes—a maize *PLTP* promoter driving a maize *BBM* (*ZmBBM*) or a barley *BBM* (*HvBBM*) combined with a maize *Axig1* promoter driving a maize *WUS* (*ZmWUS*) or a barley *WUS* (*HvWUS*) (Figure 7a). The vector generated was presented as *proZmAxig1:HvWUS+ proZmPLTP:HvBBM*. Using immature embryos as explants, *Agrobacterium*-mediated transformation was carried out. After *Agrobacterium* inoculation, callus was selected on hygromycin-containing callus induction medium and then transferred to shoot-inducing medium (SIM) for plantlet regeneration (Figure 7b). The callus proliferation rate was measured by the fresh weight of callus, and no significant change was observed after the delivery of the *proZmAxig1:HvWUS+ proZmPLTP:HvBBM* construct (Figure 7c).

Transformation of the *proZmAxig1:HvWUS + proZmPLTP:HvBBM* construct created transgenic plantlets at a frequency of 24.80%. When *proZmAxig1:ZmWUS+ proZmPLTP:ZmBBM* was used, transgenic plantlets were produced with a

mean frequency of 4.00%, compared with a frequency of 7.32% for the empty vector. In particular, the regeneration frequency increased from 24.8% to 7.32%, indicating that the effect of *HvBBM* and *HvWUS* on the transformation efficiency might depend on its promotion of plant regeneration (Table 2).

According to previous research, BBM is known to activate the LEC1-ABI3-FUS3-LEC2 network to induce somatic embryogenesis [31]. We then detected the expression of these genes downstream of *BBM*. The transcript levels of ABSCISIC ACID-INSENSITIVE3 (*ABI3*) and FUSCA3 (*FUS3*) were significantly increased in the calli co-expressing *HvBBM* and *HvWUS* (Figure 7d).

Transcriptional changes of genes regulating DNA methylation and histone modification

Epigenetic reprogramming plays an essential role in callus induction, somatic embryogenesis, and totipotency acquisition [32]. Among the putative histone methyltransferases, *SUVH4* (HORVU3Hr1G096250) was activated in both systems, and HORVU1Hr1G008690 (*SUVH9*) was only induced in the IME system. *SUVH3A* (HORVU1Hr1G068460) and *SUVH2A* (HORVU0Hr1G001190) candidate genes were downregulated in the IME system but upregulated in the ME system (Figure 8).

Two genes associated with histone acetylation were upregulated in the two systems (*RIN1*, *HAC7*), and *ELP2* (HORVU1Hr1G020620) was specifically induced in the IME system. The expression of *HAC12* (HORVU7Hr1G096240) was suppressed in the ME system (Figure 8). Two genes involved in histone deacetylation, *HDA19/703* (HORVU7Hr1G085870) and *LSD1* (HORVU6Hr1G078160), were upregulated in the IME system but remained unchanged or suppressed in the ME system.

As a critical component of epigenetic regulation, DNA methylation-related genes displayed significant changes during callus induction [32]. Six upregulated genes were found in both systems (*DRM2A*, *DRM2B*, *MET2*, *AGO6*, *CTM6*, *DMS3*). *RDM4* (HORVU4Hr1G025140) was only activated in the IME system (Figure 8). Taken together, these data suggest that epigenetic reprogramming might play an essential role in regulating gene expression during auxin-induced callus formation.

Discussion

Barley is known to be one of the most recalcitrant crops to tissue culture among the major cereals. Immature embryos are commonly used as explants in barley transformation. However, these embryos need to be dissected out individually from developing seeds, which requires significant labor and is subject to seasonal constraints. On the other hand, although mature embryos are easily accessible, it is challenging to form callus with regenerative potential using mature embryos in tissue culture. In this study, we explored global transcriptional changes during embryo-derived callus induction and identified some potential factors that might contribute to the differential responses of the two types of explants to exogenous application of auxin.

Global transcriptional changes during auxin-induced callus formation in barley

Our RNA-seq data showed that incubation of embryos on auxin-rich medium caused dramatic changes in gene expression profiles within 48 h. A total of 9330 and 11318 DEGs were found in the IME and ME systems, respectively. Most of the genes overlapped significantly, suggesting that these genes are generally associated with callus formation in different systems. Nearly 11.09% and 12.84% of exclusive DEGs were found in the IME and ME systems, respectively (Figure 2a, Figure 2b). Genes involved in various activities, such as protein phosphorylation, regulation of transcription, and the oxidation-reduction process, are enriched during immature embryo-based callus formation (Figure 2c). A previous study revealed that protein tyrosine phosphorylation might play an important regulatory role in

phytohormone-stimulated cell proliferation [33]. Furthermore, TOR kinase activated by sugar was found to phosphorylate and stabilize E2Fa proteins, which transcriptionally activate S-phase genes during callus formation [34]. Phosphorylation of E2Fa is also known to enhance its transcriptional activity [35]. These results indicate that protein phosphorylation participates in the regulation of cell proliferation during calli formation. Further, we showed that the oxidation-reduction process was significantly enriched in most comparisons. Redox homeostasis is thought to be essential for sustaining metabolism and growth as well as plant stem cell maintenance and differentiation [36]. Thioredoxin-dependent redox modification has been reported to regulate *de novo* shoot initiation via ROS homeostasis, which explains natural variation in plant regeneration [37]. Thus, it will be interesting to further explore the importance of ROS homeostasis on callus formation and regenerative competence.

Effect of auxin signaling on CIM-induced callus formation in barley

The plant hormone auxin is well established as an efficient inducer of callus formation. This study showed that the ability to form callus and its auxin signaling pathway varies between mature and immature embryos. The effect of CIM on *IAA* genes was more significant in the IME system than in the IM system, indicating that immature embryos are more sensitive to exogenous auxin supplementation. A total of 23 *IAA*, 14 *ARF*, 8 *SAUR*, 3 *YUC*, and 4 *PIN* genes were found to be differentially expressed during the callus formation process (Figure 4), supporting that auxin response and transport processes are necessary in the regulation of cell reprogramming during auxin-induced callus formation.

Studies in *Arabidopsis* show that during CIM-mediated callus formation, auxin signaling is transduced via ARF transcription factors, especially ARF7 and ARF19, to activate the expression of LBD family transcription factors [3-5], thereby inducing E2Fa to promote cell cycle reentry [38]. As such, we compared the transcription of *LBD* genes in our sequencing samples, which revealed that different combinations of *LBD16B/LBD29AB* were upregulated in the two systems (Additional file 1: Figure S7). Therefore, we suppose that LBD proteins act downstream of ARF factors to reinforce callus formation through cell cycle regulators or cell wall modification [6, 7, 38].

Embryonic genes play crucial roles in determining the acquisition of competency

We focused our analysis on key developmental genes for embryos, root and shoot meristems to determine the molecular identity of different explants and their derived calli. Root meristem regulator genes such as *PLT2* and *SHR* were shown to be significantly upregulated in the IME system, supporting that calli that develop on CIM have histological features resembling the root meristem [1, 10, 39].

Although both types of explants produce calli on auxin-rich medium, only immature embryo-derived embryonic calli acquire high regeneration potential on SIM [40]. Recent studies have shown that the embryonic nature of explants is a prerequisite for somatic cell reprogramming [41]. Ectopic overexpression of embryonic regulators or meristematic regulators induces callus formation in various plant species, illustrating that activation of undifferentiated cell fate is sufficient to drive unorganized cell proliferation [27, 29, 42-45]. Our transcriptome sequencing data showed that embryonic marker genes, such as *BBM* and *LEC1*, were rapidly induced by auxin, specifically in the IME system, and *FUS3* and *ABI3* maintained high-level transcription (Figure 5). These genes function as transcriptional activators during embryogenesis. When either of these transcription factors are ectopically expressed in *Arabidopsis*, the resulting plants produce embryonic callus on phytohormone-free medium [31, 42, 43, 45-47]. These results demonstrate that TFs involved in embryonic development are required for cell fate reprogramming, which is necessary for embryonic callus formation in CIM. As for shoot meristem genes, most of them exhibited strong or mild expression in the IME system, and only three of them were induced in the ME system (Figure 5). Notably, a *WUS* candidate gene was found to be significantly activated within 24 h of culture on CIM. Furthermore, the transcriptional level of *WUS* increased more in the IME system than in the ME system (Figure 5). The induction of *WUS*, the organizing center

regulator, has been reported to participate in the most critical events during shoot induction from the callus on SIM, which is controlled by the interaction between auxin and cytokinin [48, 49]. In contrast, auxin-induced *WUS* expression is required for the activation of the embryonic regulators *LEC1* and *LEC2* during somatic embryogenesis [50]. *LEC1* and *LEC2*, combined with *BBM* and *AGL15*, form highly interconnected transcriptional networks and promote the expression of *YUCs*, *TAA1*, and *IAA30* to modulate auxin biosynthesis and signaling [21]. Therefore, we propose that activated *WUS* expression during CIM incubation might confer pluripotency to callus cells through multiple pathways.

Overexpression of *BBM* and *WUS* enhances transformation efficiency through regulation of regeneration potential

BBM is an AP2/ERF transcription factor preferentially expressed during embryogenesis and seed development [44], while WUS is a homeodomain-containing transcription factor expressed in the stem cell organizing center of shoot meristems as well as in several callus lines [27, 28, 51]. Previous studies have demonstrated that overexpression of *BBM* induces embryonic callus in *Arabidopsis* [44] and several crop and tree species [52], and overexpression of *WUS* generates callus as well as somatic embryos in *Arabidopsis* [53]. These results indicate that the functions of *BBM* and *WUS* in promoting embryogenesis or embryonic callus formation might be conserved across dicots and can be used to increase the efficiency of callus induction. Maize *BBM* and *WUS2* have been successfully applied to stimulate transformation in maize, sorghum, sugarcane, and indica rice [54]. Considering the pleiotropic effects, such as phenotypic abnormalities and sterility, induced by the constitutive expression of maize *BBM* and *WUS2*, callus-expressed promoters (*Zm-PLTPpro*) and auxin-inducible promoters (*Zm-Axig1pro*) have been used to drive the expression of *BBM* and *WUS2*, and transgenic plants have been obtained through somatic embryos [29]. We tested this method by replacing maize genes with barley *BBM* and *WUS* and generated healthy and fertile transgenic plants. Co-expression of barley *BBM* and *WUS* significantly increased the efficiency of transformation by about three times (Figure 7). In the process of *Agrobacterium* cocultivation and subsequent selection, no significant changes were observed in callus-induction capacity, and the callus-proliferation ability reflected by fresh weight was even lower upon co-expression of *PLTPpro:HvBBM* and *Axig1pro:HvWUS* (Figure 7b). However, the plant regeneration capacity was significantly increased in the callus expressing *PLTPpro:HvBBM+Axig1pro:HvWUS*, compared to the control with the empty vector (Figure 7c, Figure 7d, Table 2). *BBM* has been shown to bind *LAFL* genes (for *LEC1/L1L*, *ABI3*, *FUS3*, and *LEC2*) to regulate their transcription, which places *BBM* upstream of other major regulators for plant embryo identity and totipotency [31]. The effect of *BBM* and *WUS* on regeneration might be explained in part by their regulatory role in the genes, such as genes encoding the B3 domain proteins ABSCISIC ACID-INSENSITIVE3 (ABI3) and FUSCA3 (FUS3) (Figure 7c), suggesting that these TFs might form a feed-forward loop to reinforce cell fate transition. Collectively, we demonstrate that the barley *WUS* and *BBM* genes can be used to stimulate barley transformation by enhancing the regenerative potential.

Epigenetic reprogramming underlying transcriptome alteration during callus induction

Accumulating evidence has shown that the transcription of many reprogramming genes during callus formation is epigenetically regulated [55]. Genetic mutations or chemical perturbations of epigenetic regulators affect callus formation and shoot regeneration in tissue culture [56]. An evolutionarily conserved protein complex POLYCOMB REPRESSIVE COMPLEX 2 (PRC2)- mediated histone H3 lysine 27 trimethylation (H3K27me3) is thought to maintain the repressive status of target genes [55], including genes encoding embryonic regulators, such as *LEC2* and *BBM*, to prevent the ectopic onset of embryogenesis and callus formation [57, 58]. A mechanism to activate PRC2-repressed reprogramming regulator genes is to reduce the level of H3K27me3 through histone demethylase. Two candidate genes, HORVU3Hr1G096250 and HORVU7Hr1G073410, encoding proteins similar to *Arabidopsis* SUVH4 and FIS3, respectively, were found to be activated in the two systems (Figure 8), indicating their regulatory roles in callus induction. Furthermore, HORVU1Hr1G008690, encoding a homolog of *SUVH9* in *Arabidopsis*—known as a SET domain

protein that acts as a histone methyltransferase—was significantly upregulated in the IME system alone (Figure 8). We specifically detected the induction of the histone acetylation-related gene *ELP2* (HORVU1Hr1G020620) in the IME system (Figure 8), raising the possibility that histone acetylation may help to activate gene expression. Meanwhile, two histone deacetylase genes, *HDT2* (HORVU1Hr1G095140) and *HDT3* (HORVU1Hr1G095140), were specifically upregulated in the IME system. This is consistent with a previous study, which reported that the rice histone deacetylase OsHDA710 regulates callus formation by suppressing repressive OsARFs via histone deacetylation in mature rice embryos [59].

DNA methylation is another important component of epigenetic regulation, and DNA methyltransferase genes display dynamic expression changes after callus induction [32]. Two of them, *DRM2A* (HORVU0Hr1G018360) and *CMT2* (HORVU6Hr1G089250), were significantly activated in the ME system. In contrast, *RDM4* (HORVU4Hr1G025140) was only activated in the IME system (Figure 8). In addition to DNA methylation and histone modification, auxin has been reported to rewire chromatin accessibility dynamics to promote the acquisition of plant cell totipotency in plant somatic embryogenesis [41]. Further investigation is necessary to understand the molecular link between epigenetic regulation and cell reprogramming during callus formation and shoot regeneration.

Conclusions

Through a detailed analysis of gene expression profiles during barley embryo-derived callus induction, we found that more auxin-induced genes were associated with auxin response and transport in the IME system than in the IM system. Embryonic genes *BBM*, *LEC1*, and *FUS3* and shoot and root meristem genes *WUS* and *PLT2* displayed differential expression patterns between the two systems, indicating their crucial roles in determining the acquisition of competency. Furthermore, epigenetic modifications may participate in regulating the expression state of genes in different explants and their responses to callus induction (Figure 9). *HvBBM* and *HvWUS* might be used as potential targets to improve barley transformation efficiency.

Methods

Plant materials and tissue culture

Barley plants (*Hordeum vulgare* L. cv. Golden Promise) were grown under natural conditions (from November to May) at the Agricultural Experiment Station of Zhejiang University, Hangzhou, Zhejiang Province, China. The immature seeds (14 days post-pollination) were surface-sterilized for 1 min in 75% (v/v) ethanol, followed by 20 min in 20% (v/v) sodium hypochlorite, and then rinsed five times with sterilized distilled water. The mature seeds were soaked in 50% sulfuric acid for 2 h to remove the seed coat before surface sterilization. After removing the embryonic axis, immature embryos (IME) and mature embryos (ME) were placed, with the scutellum facing upwards, in the callus induction medium [60] in a growth chamber at 24 °C in the dark for callus induction. The MEs and IMEs were cultured in three biological replicates; each replicate consisted of four plates and each plate contained 30 embryos. The immature embryo samples were harvested at 0 h, 24 h, and 48 h after culture in CIM. The mature embryos were harvested at 0 h and 24 h after culture in CIM. Then, they were snap-frozen in liquid nitrogen and stored at −80 °C until RNA extraction.

RNA isolation, library construction, and sequencing

A cDNA library was constructed from the pooled RNA of immature and mature barley embryos. Using the Illumina paired-end RNA-seq approach, the transcriptome was then sequenced, this generated a total of 756 million paired-end reads, yielding 114 gigabases (Gb) of sequences. Prior to assembly, the low-quality reads (reads containing

sequencing adaptors, reads containing sequencing primer, and nucleotides with a q quality score lower than 20) were removed, resulting in 617 million bp of cleaned, paired-end reads.

Reads of samples A and B were aligned to the Ensembl (ftp://ftp.ensemblgenomes.org/pub/release-43/plants/fasta/hordeum_vulgare/dna/Hordeum_vulgare.IBS Cv2.dna.toplevel.fa.gz) barley reference genome using the HISAT package [61], which initially removes a portion of the reads—based on quality information accompanying each read—and then maps the reads to the reference genome. HISAT allows multiple alignments per read (up to 20 by default) and a maximum of two mismatches when mapping the reads to the reference, and builds a database of potential splice junctions and confirms these by comparing the previously unmapped reads against the database of putative junctions. Then, sequence-dependent bias and amplification noise were removed using UMI-tools [62].

The mapped reads of each sample were assembled using StringTie [63]. Then, all transcriptomes from samples were merged to reconstruct a comprehensive transcriptome using Perl scripts. After the final transcriptome was generated, StringTie and edgeR were used to estimate the expression levels of all transcripts. StringTie was used to predict mRNA expression levels by calculating FPKM. The differentially expressed mRNAs and genes were selected with $|\log_2 \text{fold change}| \geq 1$ and with statistical significance of pvalue < 0.05, using the R package edgeR [64].

Real-time qRT-PCR

Total RNA from barley tissues was extracted using RNAiso Plus (TaKaRa, Dalian, China), and 1 μg of it was used for first-strand cDNA synthesis using ReverTra Ace qPCR RT Kit (Toyobo, Shanghai, China). qRT-PCR was performed on the Mastercycler Ep Realplex2 system (Eppendorf, Hamburg, Germany) using a SYBR Green Master Kit (Roche, Basel, Switzerland). Relative transcript levels were calculated using the $^{\Delta\Delta}$Ct method, and *ACTIN* was used as a reference.

Vector construction and *Agrobacterium*-mediated barley transformation

The arrangement of expression cassettes within the T-DNA of plasmids used in this study is shown in Figure 7a. The *proZmPLTP:ZmBBM+proZmAxig1:ZmWUS2* construct contained two cassettes; the first one included a maize phospholipid transferase promoter (*proZmPLTP*) driving *ZmBBM* with a Nos terminator, and the second one included a maize *Axig1* promoter (*proZmAxig1*) driving *WUS2* with a Nos terminator [30]. For the *proZmPLTP:HvBBM+proZmAxig1:HvWUS2* construct, the promoters used were identical to those in the *proZmPLTP:ZmBBM+proZmAxig1:ZmWUS2* construct, with the homologous genes in barley replacing *ZmBBM* and *ZmWUS2*. All the promoters and genes were amplified by PCR, and the PCR products were assembled using an infusion kit (TaKaRa, Dalian, China), and then sub-cloned in *pCAMBIA1305*. The primers used in this study are listed in Supplemental Table S2. The clones used for vector construction were verified by sequencing. The constructs described were electroporated into *Agrobacterium tumefaciens* strain EHA105. Transformation was performed through the infection of immature embryos (IMEs)-derived scutellum of barley with *Agrobacterium*, followed by selection of transgenic tissues on media containing 50 mg L^{-1} hygromycin [65]. Transformation frequency was defined as the number of treated immature embryos that produced hygromycin-resistant T_0 plants.

Abbreviations

IME: Immature embryo; ME: Mature embryo; DEGs: Differential expressed genes; CIM: Callus-inducing medium; SIM: Shoot-inducing medium; WOX5: WUSCHEL-RELATED HOMEOBOX5; SHR: SHORT ROOT; ARF: AUXIN RESPONSE FACTOR; LBD: LATERAL ORGAN BOUNDARIES DOMAIN; CUC: CUP-SHAPED COTYLEDON; PLTs: PLETHORA proteins; ABI3: ABSCISIC ACID-INSENSITIVE 3; FUS3: FUSCA3; PRC2: POLYCOMB REPRESSIVE COMPLEX 2; SAM: Shoot apical meristem; RAM: Root apical meristem; DPA: Days post-anthesis. qRT-PCR: Quantitative reverse transcription PCR; GO:

Gene ontology; UMI: Unique molecular identifier; TFs: Transcription factors; BBM: BABY BOOM; WUS: WUSCHEL; LEC1: LEAFY COTYLEDON 1; IAA: INDOLEACETIC ACID; SAUR: SMALL AUXIN UP RNA; PIN: PIN-FORMED; YUC: YUCCA; GO: Gene ontology;

Declarations

Ethics approval and consent to participate

Not applicable.

Consent for publication

Not applicable.

Availability of data and materials

All data generated or analyzed during this study are included in this published article and its additional files.

Competing interests

The authors declare that they have no competing interests.

Funding

This work was supported by the China Agriculture Research System (CARS-05-05A) and Zhejiang Provincial Natural Science Foundation (grant No. LGN18C130001).

Authors' contributions

JQS and CLZ prepared samples for RNA sequencing, and performed qRT-PCR detection. JQS, ZHZ and XPL performed transformation and tissue culture. JQS and CLZ gave a contribution to bioinformatics analysis. NH designed and coordinated the work, and wrote the manuscript with JQS. HWB, JHW and MYZ contributed to the design and discussion of the work, and assisted in drafting the manuscript. All authors read and approved the final manuscript.

Acknowledgements

Not applicable.

References

1. Sugimoto K, Jiao Y, Meyerowitz EM. Arabidopsis regeneration from multiple tissues occurs via a root development pathway. Dev Cell. 2010;18:463-471.
2. Efroni I, Mello A, Nawy T, Ip PL, Rahni R, DelRose N, Powers A, Satija R, Birnbaum KD. Root Regeneration Triggers an Embryo-like Sequence Guided by Hormonal Interactions. Cell. 2016;165:1721-1733.
3. Fukaki H, Nakao Y, Okushima Y, Theologis A, Tasaka M. Tissue-specific expression of stabilized SOLITARY-ROOT/IAA14 alters lateral root development in Arabidopsis. Plant J. 2005;44:382-395.
4. Fan M, Xu C, Xu K, Hu Y. LATERAL ORGAN BOUNDARIES DOMAIN transcription factors direct callus formation in Arabidopsis regeneration. Cell Res. 2012;22:1169-1180.

5. Okushima Y, Fukaki H, Onoda M, Theologis A, Tasaka M. ARF7 and ARF19 regulate lateral root formation via direct activation of LBD/ASL genes in Arabidopsis. Plant Cell. 2007;19:118-130.
6. Lee HW, Kim MJ, Kim NY, Lee SH, Kim J. LBD18 acts as a transcriptional activator that directly binds to the EXPANSIN14 promoter in promoting lateral root emergence of Arabidopsis. Plant J. 2013;73:212-224.
7. Xu C, Cao H, Xu E, Zhang S, Hu Y. Genome-Wide Identification of Arabidopsis LBD29 Target Genes Reveals the Molecular Events behind Auxin-Induced Cell Reprogramming during Callus Formation. Plant Cell Physiol. 2018;59:744-755.
8. Xu C, Cao H, Zhang Q, Wang H, Xin W, Xu E, Zhang S, Yu R, Yu D, Hu Y. Control of auxin-induced callus formation by bZIP59-LBD complex in Arabidopsis regeneration. Nat Plants. 2018;4:108-115.
9. Daimon Y, Takabe K, Tasaka M. The CUP-SHAPED COTYLEDON genes promote adventitious shoot formation on calli. Plant Cell Physiol. 2003;44:113-121.
10. Kareem A, Durgaprasad K, Sugimoto K, Du Y, Pulianmackal AJ, Trivedi ZB, Abhayadev PV, Pinon V, Meyerowitz EM, Scheres B *et al*. PLETHORA Genes Control Regeneration by a Two-Step Mechanism. Curr Biol. 2015;25:1017-1030.
11. Guo F, Zhang H, Liu W, Hu X, Han N, Qian Q, Xu L, Bian H. Callus initiation from root explants employs different strategies in rice and Arabidopsis. Plant Cell Physiol. 2018;59:1782-1789.
12. Tingay S, McElroy D, Kalla R, Fieg S, Wang M, Thornton S, Brettell R. Agrobacterium tumefaciens-mediated barley transformation. The Plant Journal. 1997;11:1369-1376.
13. Holme IB, Brinch-Pedersen H, Lange M, Holm PB. Transformation of different barley (Hordeum vulgare L.) cultivars by Agrobacterium tumefaciens infection of in vitro cultured ovules. Plant Cell Rep. 2008;27:1833-1840.
14. Shim YS, Pauls KP, Kasha KJ. Transformation of isolated barley (Hordeum vulgare L.) microspores: II. Timing of pretreatment and temperatures relative to results of bombardment. Genome. 2009;52:175-190.
15. Shim YS, Pauls KP, Kasha KJ. Transformation of isolated barley (Hordeum vulgare L.) microspores: I. the influence of pretreatments and osmotic treatment on the time of DNA synthesis. Genome. 2009;52:166-174.
16. Kumlehn J, Serazetdinova L, Hensel G, Becker D, Loerz H. Genetic transformation of barley (Hordeum vulgare L.) via infection of androgenetic pollen cultures with Agrobacterium tumefaciens. Plant Biotechnol J. 2006;4:251-261.
17. Lim WL, Collins HM, Singh RR, Kibble NAJ, Yap K, Taylor J, Fincher GB, Burton RA. Method for hull-less barley transformation and manipulation of grain mixed-linkage beta-glucan. J Integr Plant Biol. 2018;60:382-396.
18. Hisano H, Sato K. Genomic regions responsible for amenability to Agrobacterium-mediated transformation in barley. Sci Rep. 2016;6:37505.
19. Hisano H, Meints B, Moscou MJ, Cistue L, Echavarri B, Sato K, Hayes PM. Selection of transformation-efficient barley genotypes based on TFA (transformation amenability) haplotype and higher resolution mapping of the TFA loci. Plant Cell Rep. 2017;36:611-620.
20. Orman-Ligeza B, Harwood W, Hedley PE, Hinchcliffe A, Macaulay M, Uauy C, Trafford K. TRA1: A Locus Responsible for Controlling Agrobacterium-Mediated Transformability in Barley. Front Plant Sci. 2020;11:355.
21. Ikeuchi M, Favero DS, Sakamoto Y, Iwase A, Coleman D, Rymen B, Sugimoto K. Molecular Mechanisms of Plant Regeneration. Annu Rev Plant Biol. 2019;70:377-406.
22. Ikeuchi M, Sugimoto K, Iwase A. Plant callus: mechanisms of induction and repression. Plant Cell. 2013;25:3159-3173.
23. Skoog F, Miller CO. Chemical regulation of growth and organ formation in plant tissues cultured in vitro. Symp Soc Exp Biol. 1957;11:118-130.
24. Feher A. Somatic embryogenesis - Stress-induced remodeling of plant cell fate. Bba-Gene Regul Mech. 2015;1849:385-402.

25. Valvekens D, Vanmontagu M, Vanlijsebettens M. Agrobacterium-Tumefaciens-Mediated Transformation of Arabidopsis-Thaliana Root Explants by Using Kanamycin Selection. P Natl Acad Sci USA. 1988;85:5536-5540.
26. Che P, Lall S, Howell SH. Developmental steps in acquiring competence for shoot development in Arabidopsis tissue culture. Planta. 2007;226:1183-1194.
27. Mayer KF, Schoof H, Haecker A, Lenhard M, Jurgens G, Laux T. Role of WUSCHEL in regulating stem cell fate in the Arabidopsis shoot meristem. Cell. 1998;95:805-815.
28. Laux T, Mayer KFX, Berger J, Jurgens G. The WUSCHEL gene is required for shoot and floral meristem integrity in Arabidopsis. Development. 1996;122:87-96.
29. Lowe K, Wu E, Wang N, Hoerster G, Hastings C, Cho MJ, Scelonge C, Lenderts B, Chamberlin M, Cushatt J *et al*. Morphogenic Regulators Baby boom and Wuschel Improve Monocot Transformation. Plant Cell. 2016;28:1998-2015.
30. Lowe K, La Rota M, Hoerster G, Hastings C, Wang N, Chamberlin M, Wu E, Jones T, Gordon-Kamm W. Rapid genotype "independent" Zea mays L. (maize) transformation via direct somatic embryogenesis. In Vitro Cell Dev Biol Plant. 2018;54:240-252.
31. Horstman A, Li M, Heidmann I, Weemen M, Chen B, Muino JM, Angenent GC, Boutilier K. The BABY BOOM Transcription Factor Activates the LEC1-ABI3-FUS3-LEC2 Network to Induce Somatic Embryogenesis. Plant Physiol. 2017;175:848-857.
32. Stroud H, Ding B, Simon SA, Feng SH, Bellizzi M, Pellegrini M, Wang GL, Meyers BC, Jacobsen SE. Plants regenerated from tissue culture contain stable epigenome changes in rice. Elife. 2013;2.
33. Huang HJ, Lin YM, Huang DD, Takahashi T, Sugiyama M. Protein tyrosine phosphorylation during phytohormone-stimulated cell proliferation in Arabidopsis Hypocotyls. Plant Cell Physiol. 2003;44:770-775.
34. Lee K, Seo PJ. Arabidopsis TOR signaling is essential for sugar-regulated callus formation. J Integr Plant Biol. 2017;59:742-746.
35. Xiong Y, McCormack M, Li L, Hall Q, Xiang C, Sheen J. Glucose-TOR signalling reprograms the transcriptome and activates meristems. Nature. 2013;496:181-186.
36. Zeng J, Dong Z, Wu H, Tian Z, Zhao Z. Redox regulation of plant stem cell fate. EMBO J. 2017;36:2844-2855.
37. Zhang H, Zhang TT, Liu H, Shi Y, Wang M, Bie XM, Li XG, Zhang XS. Thioredoxin-Mediated ROS Homeostasis Explains Natural Variation in Plant Regeneration. Plant Physiol. 2018;176:2231-2250.
38. Berckmans B, Vassileva V, Schmid SP, Maes S, Parizot B, Naramoto S, Magyar Z, Alvim Kamei CL, Koncz C, Bogre L *et al*. Auxin-dependent cell cycle reactivation through transcriptional regulation of Arabidopsis E2Fa by lateral organ boundary proteins. Plant Cell. 2011;23:3671-3683.
39. Bustillo-Avendano E, Ibanez S, Sanz O, Sousa Barros JA, Gude I, Perianez-Rodriguez J, Micol JL, Del Pozo JC, Moreno-Risueno MA, Perez-Perez JM. Regulation of Hormonal Control, Cell Reprogramming, and Patterning during De Novo Root Organogenesis. Plant Physiol. 2018;176:1709-1727.
40. Ganeshan S, Baga M, Harvey BL, Rossnagel BG, Scoles GJ, Chibbar RN. Production of multiple shoots from thidiazuron-treated mature embryos and leaf-base/apical meristems of barley (Hordeum vulgare). Plant Cell Tiss Org. 2003;73:57-64.
41. Wang FX, Shang GD, Wu LY, Xu ZG, Zhao XY, Wang JW. Chromatin Accessibility Dynamics and a Hierarchical Transcriptional Regulatory Network Structure for Plant Somatic Embryogenesis. Developmental Cell. 2020;54:742-757.
42. Lotan T, Ohto M, Yee KM, West MA, Lo R, Kwong RW, Yamagishi K, Fischer RL, Goldberg RB, Harada JJ. Arabidopsis LEAFY COTYLEDON1 is sufficient to induce embryo development in vegetative cells. Cell.

1998;93:1195-1205.

43. Stone SL, Kwong LW, Yee KM, Pelletier J, Lepiniec L, Fischer RL, Goldberg RB, Harada JJ. LEAFY COTYLEDON2 encodes a B3 domain transcription factor that induces embryo development. Proc Natl Acad Sci U S A. 2001;98:11806-11811.
44. Boutilier K, Offringa R, Sharma VK, Kieft H, Ouellet T, Zhang L, Hattori J, Liu CM, van Lammeren AA, Miki BL *et al*. Ectopic expression of BABY BOOM triggers a conversion from vegetative to embryonic growth. Plant Cell. 2002;14:1737-1749.
45. Braybrook SA, Stone SL, Park S, Bui AQ, Le BH, Fischer RL, Goldberg RB, Harada JJ. Genes directly regulated by LEAFY COTYLEDON2 provide insight into the control of embryo maturation and somatic embryogenesis. Proc Natl Acad Sci U S A. 2006;103:3468-3473.
46. Harding EW, Tang W, Nichols KW, Fernandez DE, Perry SE. Expression and maintenance of embryogenic potential is enhanced through constitutive expression of AGAMOUS-Like 15. Plant Physiol. 2003;133:653-663.
47. Stone SL, Braybrook SA, Paula SL, Kwong LW, Meuser J, Pelletier J, Hsieh TF, Fischer RL, Goldberg RB, Harada JJ. Arabidopsis LEAFY COTYLEDON2 induces maturation traits and auxin activity: Implications for somatic embryogenesis. Proc Natl Acad Sci U S A. 2008;105:3151-3156.
48. Gallois JL, Nora FR, Mizukami Y, Sablowski R. WUSCHEL induces shoot stem cell activity and developmental plasticity in the root meristem. Genes Dev. 2004;18:375-380.
49. Cheng ZJ, Wang L, Sun W, Zhang Y, Zhou C, Su YH, Li W, Sun TT, Zhao XY, Li XG *et al*. Pattern of auxin and cytokinin responses for shoot meristem induction results from the regulation of cytokinin biosynthesis by AUXIN RESPONSE FACTOR3. Plant Physiol. 2013;161:240-251.
50. Ma YF, Miotk A, Sutikovic Z, Ermakova O, Wenzl C, Medzihradszky A, Gaillochet C, Forner J, Utan G, Brackmann K *et al*. WUSCHEL acts as an auxin response rheostat to maintain apical stem cells in Arabidopsis. Nature Communications. 2019;10.
51. Iwase A, Mitsuda N, Koyama T, Hiratsu K, Kojima M, Arai T, Inoue Y, Seki M, Sakakibara H, Sugimoto K *et al*. The AP2/ERF Transcription Factor WIND1 Controls Cell Dedifferentiation in Arabidopsis. Current Biology. 2011;21:508-514.
52. El Ouakfaoui S, Schnell J, Abdeen A, Colville A, Labbe H, Han S, Baum B, Laberge S, Miki B. Control of somatic embryogenesis and embryo development by AP2 transcription factors. Plant Mol Biol. 2010;74:313-326.
53. Zuo JR, Niu QW, Frugis G, Chua NH. The WUSCHEL gene promotes vegetative-to-embryonic transition in Arabidopsis. Plant Journal. 2002;30:349-359.
54. Lowe K, La Rota M, Hoerster G, Hastings C, Wang N, Chamberlin M, Wu E, Jones T, Gordon-Kamm W. Rapid genotype "independent" Zea mays L. (maize) transformation via direct somatic embryogenesis. In Vitro Cell Dev-Pl. 2018;54:240-252.
55. Ikeuchi M, Iwase A, Rymen B, Harashima H, Shibata M, Ohnuma M, Breuer C, Morao AK, de Lucas M, De Veylder L *et al*. PRC2 represses dedifferentiation of mature somatic cells in Arabidopsis. Nature Plants. 2015;1:1-7.
56. Lee K, Seo PJ. Dynamic Epigenetic Changes during Plant Regeneration. Trends in Plant Science. 2018;23:235-247.
57. Bouyer D, Roudier F, Heese M, Andersen ED, Gey D, Nowack MK, Goodrich J, Renou JP, Grini PE, Colot V *et al*. Polycomb Repressive Complex 2 Controls the Embryo-to-Seedling Phase Transition. Plos Genetics. 2011;7.
58. Bratzel F, Lopez-Torrejon G, Koch M, Del Pozo JC, Calonje M. Keeping Cell Identity in Arabidopsis Requires PRC1 RING-Finger Homologs that Catalyze H2A Monoubiquitination. Current Biology. 2010;20:1853-1859.
59. Zhang H, Guo F, Qi P, Huang Y, Xie Y, Xu L, Han N, Xu L, Bian H. OsHDA710-mediated Histone Deacetylation Regulates Callus Formation of Rice Mature Embryo. Plant Cell Physiol. 2020;61:1646-1660.

60. Harwood WA. A Protocol for High-Throughput Agrobacterium-Mediated Barley Transformation. Methods in Molecular Biology. 2014;1099:251-260.
61. Kim D, Landmead B, Salzberg SL. HISAT: a fast spliced aligner with low memory requirements. Nat Methods. 2015;12:357-360.
62. Smith T, Heger A, Sudbery I. UMI-tools: modeling sequencing errors in Unique Molecular Identifiers to improve quantification accuracy. Genome Res. 2017;27:491-499.
63. Pertea M, Pertea GM, Antonescu CM, Chang TC, Mendell JT, Salzberg SL. StringTie enables improved reconstruction of a transcriptome from RNA-seq reads. Nat Biotechnol. 2015;33:290-295.
64. Robinson MD, McCarthy DJ, Smyth GK. edgeR: a Bioconductor package for differential expression analysis of digital gene expression data. Bioinformatics. 2010;26:139-140.
65. Harwood WA. A protocol for high-throughput Agrobacterium-mediated barley transformation. Methods Mol Biol. 2014;1099:251-260.

Tables

Table 1 Statistics of the total reads mapped to the reference genome from five libraries

Sample		Valid reads	Mapped reads	Unique Mapped reads	Multi Mapped reads	PE Mapped reads	Reads map to sense strand	Reads map to antisense strand
IME_0h	1	50,508,092	46,525,933 (92.12%)	34,881,919 (69.06%)	11,644,014 (23.05%)	43,551,514 (86.23%)	19,365,009 (38.34%)	19,429,297 (38.47%)
	2	50,725,082	46,718,943 (92.10%)	35,343,451 (69.68%)	11,375,492 (22.43%)	43,728,232 (86.21%)	19,462,644 (38.37%)	19,535,977 (38.51%)
	3	51,346,982	47,181,924 (91.89%)	35,467,427 (69.07%)	11,714,497 (22.81%)	43,783,770 (85.27%)	19,463,881 (37.91%)	19,543,884 (38.06%)
IME_24h	1	42,482,012	39,600,956 (93.22%)	29,826,685 (70.21%)	9,774,271 (23.01%)	37,024,224 (87.15%)	16,758,583 (39.45%)	16,767,271 (39.47%)
	2	46,361,390	43,046,755 (92.85%)	32,242,450 (69.55%)	10,804,305 (23.30%)	40,242,720 (86.80%)	17,995,697 (38.82%)	18,002,730 (38.83%)
	3	49,289,192	45,811,254 (92.94%)	34,207,322 (69.40%)	11,603,932 (23.54%)	42,805,810 (86.85%)	19,165,613 (38.88%)	19,175,961 (38.91%)
IME_48h	1	50,064,794	45,466,924 (90.82%)	33,987,373 (67.89%)	11,479,551 (22.93%)	42,464,724 (84.82%)	18,904,502 (37.76%)	18,898,466 (37.75%)
	2	52,617,624	48,950,150 (93.03%)	36,748,315 (69.84%)	12,201,835 (23.19%)	45,431,552 (86.34%)	20,474,061 (38.91%)	20,481,498 (38.93%)
	3	51,022,778	47,542,104 (93.18%)	35,553,488 (69.68%)	11,988,616 (23.50%)	44,136,992 (86.50%)	19,950,036 (39.10%)	19,953,944 (39.11%)
ME_0h	1	44,726,072	41,111,321 (91.92%)	30,307,401 (67.76%)	10,803,920 (24.16%)	38,293,348 (85.62%)	17,002,182 (38.01%)	17,013,183 (38.04%)
	2	48,998,490	44,815,937 (91.46%)	33,012,162 (67.37%)	11,803,775 (24.09%)	41,883,774 (85.48%)	18,641,797 (38.05%)	18,639,916 (38.04%)
	3	51,294,828	46,955,145 (91.54%)	34,689,826 (67.63%)	12,265,319 (23.91%)	43,865,372 (85.52%)	19,319,169 (37.66%)	19,322,335 (37.67%)
ME_24h	1	49,828,700	46,579,576 (93.48%)	34,747,312 (69.73%)	11,832,264 (23.75%)	43,617,610 (87.54%)	19,371,793 (38.88%)	19,360,153 (38.85%)
	2	51,117,256	47,940,378 (93.79%)	35,939,931 (70.31%)	12,000,447 (23.48%)	44,326,868 (86.72%)	20,082,418 (39.29%)	20,078,786 (39.28%)
	3	49,956,734	46,882,189 (93.85%)	34,969,303 (70.00%)	11,912,886 (23.85%)	43,922,646 (87.92%)	19,662,673 (39.36%)	19,650,293 (39.33%)

Sample: sequencing library name; Valid reads: the number of reads after UID deduplication; Mapped reads: the number of reads that can be compared to the genome; Unique Mapped reads: the number of reads that can only be uniquely aligned to a position in the genome; Multi mapped reads: the number of reads that can be compared to multiple positions in the genome; PE Mapped reads: pair-end sequencing reads are paired to the genome reads; Reads map to sense strand: after UMI deduplication, read comparison to the statistics of the sense strand of the genome; Reads map to antisense strand: after UMI deduplication, the statistics of read alignment to the negative sense strand of the genome; Non-splice reads: after UMI deduplication, read can compare end-to-end to the genomic region, and compare statistics for the entire segment; Splice reads: after UMI deduplication, read cannot end-to-end comparison to the genomic region, which is a segmented comparison statistics.

Table 2 The effect of *BBM* and *WUS* on *Agrobacterium*-mediated barley transformation using immature embryos as explants.

Developmental Gene Expression Cassettes	No. of explants	No. of regenerated plants	Regeneration Freq.	No. of T_0	Transformation Freq.
pCAMBIA1305 EV	615	48	7.80%	45	7.32%
proZmPLTP:HvBBM +proZmAxig1:HvWUS	575	27	4.7%	23	4.00%
proZmPLTP:HvBBM +proZmAxig1:HvWUS	613	155	25.29%	152	24.8%

Agrobacterium (strain EHA105)-mediated barley transformation was performed using immature embryos as explants. The *proZmPLTP:HvBBM+proZmAxig1:HvWUS* construct contains two cassettes, the first one included a maize phospholipid transferase promoter (*proZmPLTP)* driving *HvBBM*, the second one included maize *Axig1* promoter (*proZmAxig1*) driving the *HvWUS*. *pCAMBIA1305* empty vector (EV) was used as control. Regeneration Freq. was estimated as No. of regenerated plants divided by No. of explants, and transformation frequency was calculated as No. of T_0 divided by No. of explants.

Additional Files

Additional file 1

Table S1. Statistics of the total reads from five libraries.

Table S2. Summary of data cleaning and length distribution of tags

Figure S1. Pearson correlation between samples.

Figure S2. Gene Ontology (GO) enrichment analysis of differentially expressed genes.

Figure S3. KEGG analysis of differentially expressed genes.

Figure S4. Expression of a set of callus-inducing medium (CIM)-induced transcription factors during immature and mature embryo-derived callus formation.

Figure S5. Phylogenetic tree of BBM and WUS among barley and other species.

Figure S6. Expression analysis of candidate *LEC1* gene during callus formation.

Figure S7. Expression analysis of candidate LBD genes potentially associated with callus formation in barley.

Table S3. List of primers used in this study.

Additional file 2. Supplementary raw data.

Figures

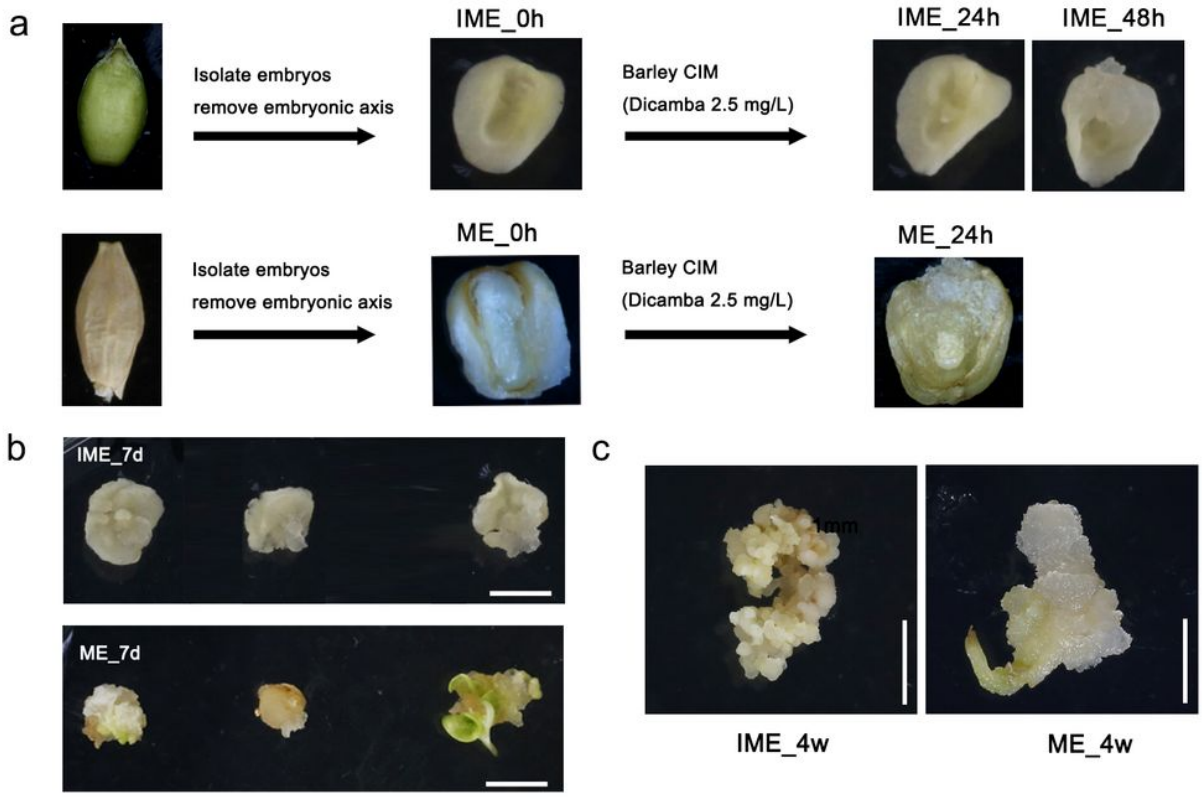

Figure 1

Characteristics of callus formed in immature (IME) and mature (ME) embryos. a: Schematic diagram of sample collection for RNA-seq analysis. After surface-sterilization of mature seeds and embryonic axis removal from immature seeds (14 days post-anthesis), embryos were isolated and cultured on CIM. The samples for RNA-seq were collected at three-time points from immature embryo-derived callus (IME_0h, IME_24h and IME_48h), and two-time points from mature embryo-derived callus (ME_0h and ME_24h). b: Scutellum-induced callus formation in barley cv. Golden Promise after 7 days of culture. Bar =500 μm. c: Scutellum-induced callus formation in barley cv. Golden Promise after 4 weeks of culture. Bar =500 mm.

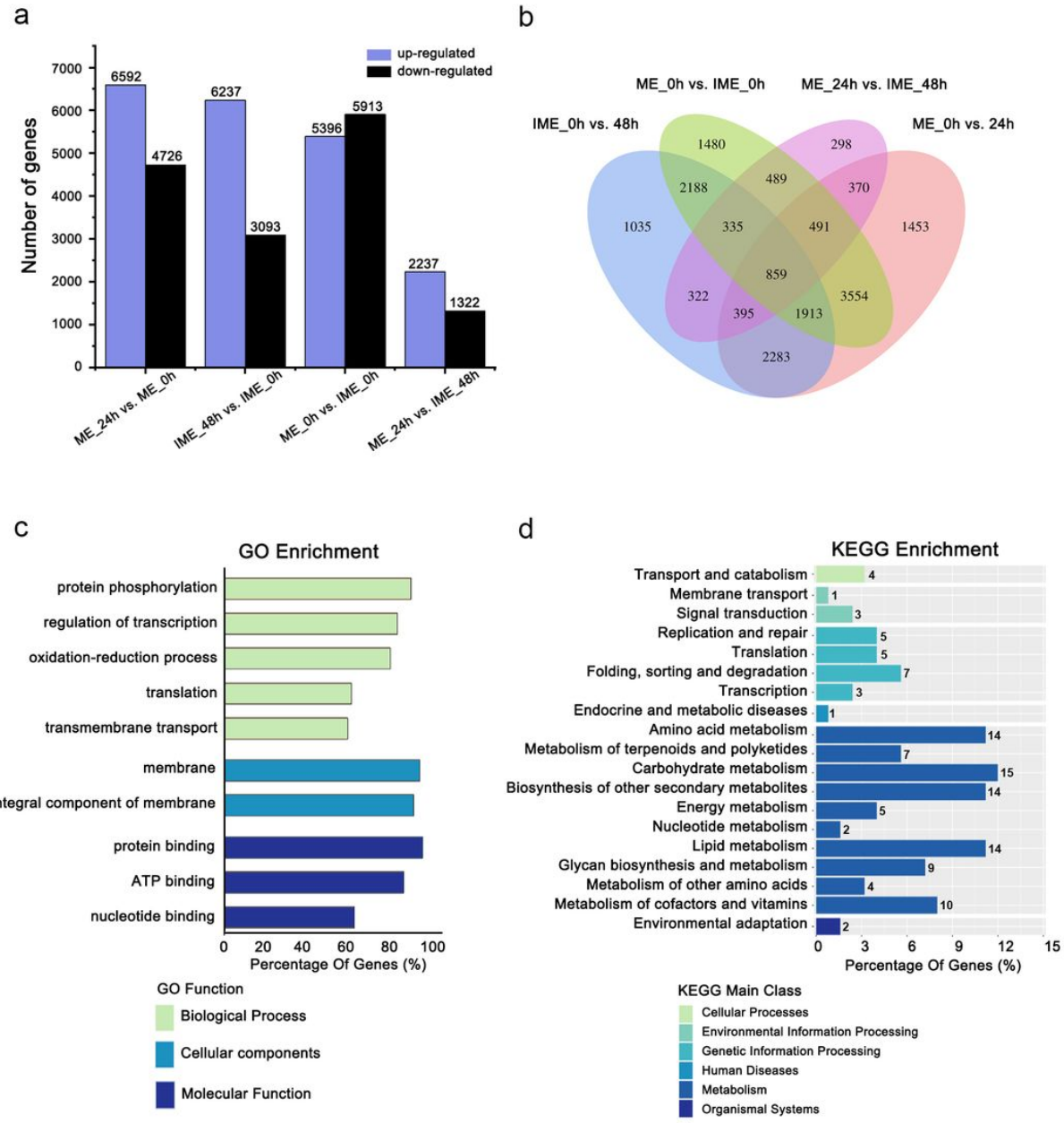

Figure 2

Differentially expressed genes in different groups. a: The number of DEGs up-or downregulated during embryo-derived callus formation and between two callus induction systems. b: Venn diagram showing overlap and specific DEGs between two samples. c-d: The top 10 most enriched Gene Ontology (GO) (c) and the top 19 most enriched KEGG (d) categories among up- and downregulated genes at any given time point. Highly redundant GO and KEGG categories were manually removed.

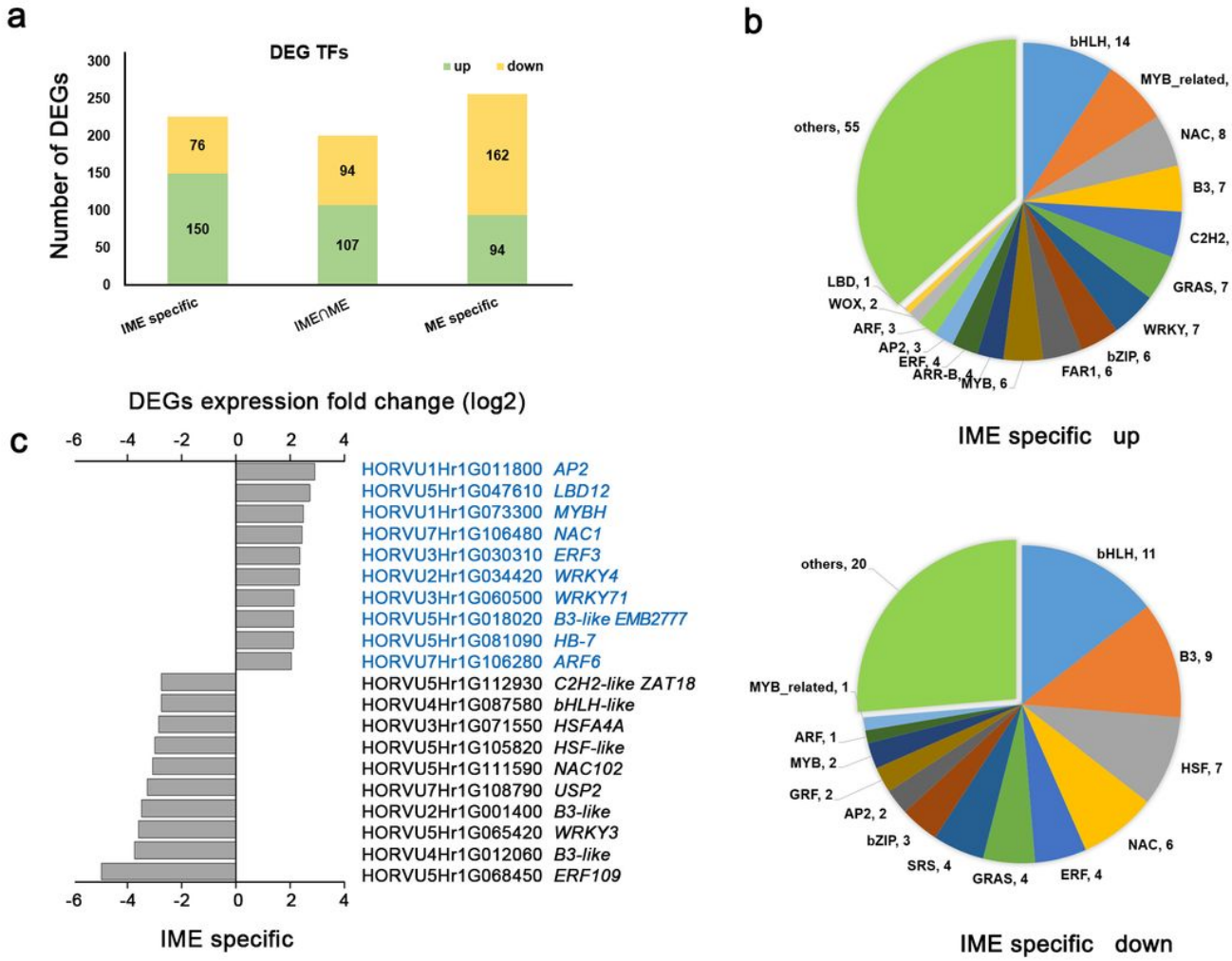

Figure 3

Expression of a set of callus-inducing medium (CIM)-induced transcription factors during immature and mature embryo-derived callus formation. a: The number of differentially expressed TFs detected only in the IME system (IME specific), only in the ME system (ME specific), and in both systems (IME∩ME). b: Upregulated (upper) and downregulated (lower) TF families specific to the IME system. Numbers represent the gene members associated with a given TF family. c: The top 10 differentially expressed TFs in the IME system (IME specific). Genes marked in blue are upregulated TFs, and transcription factors marked in black are downregulated.

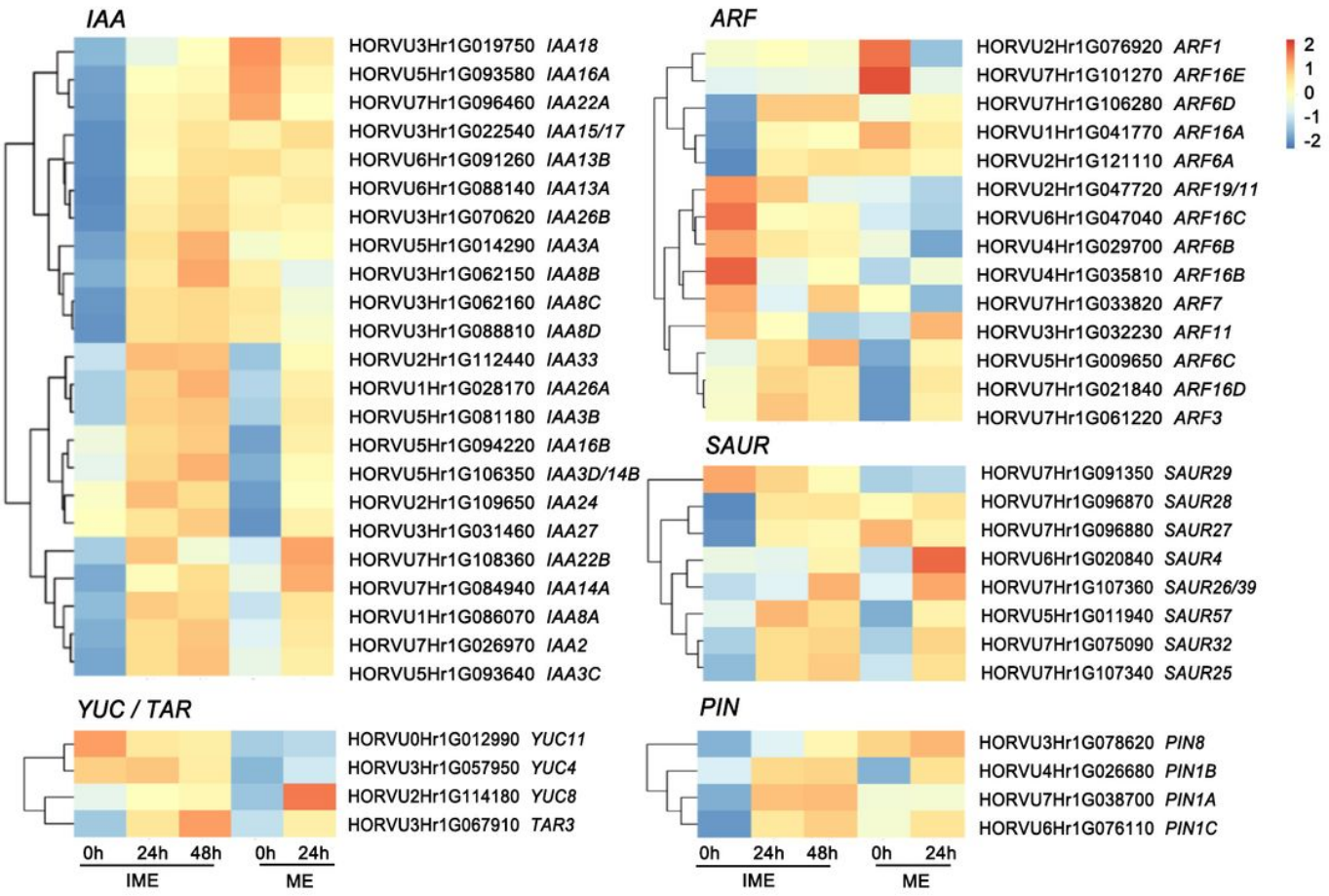

Figure 4

Expression of genes involved in the auxin pathway during callus-inducing medium (CIM)-mediated callus formation. The expression levels were visualized by using OmicStudio tools at https://www.omicstudio.cn/tool based on RNA-seq datasets (Additional file 2: Supplementary raw data). Numbers beneath the heat map indicate the relative expression intensities, and the higher expression intensities are indicated by more reddish colors. Genes are grouped by auxin response, biosynthesis, and transport genes. Note that only genes with RPKM>1 are shown.

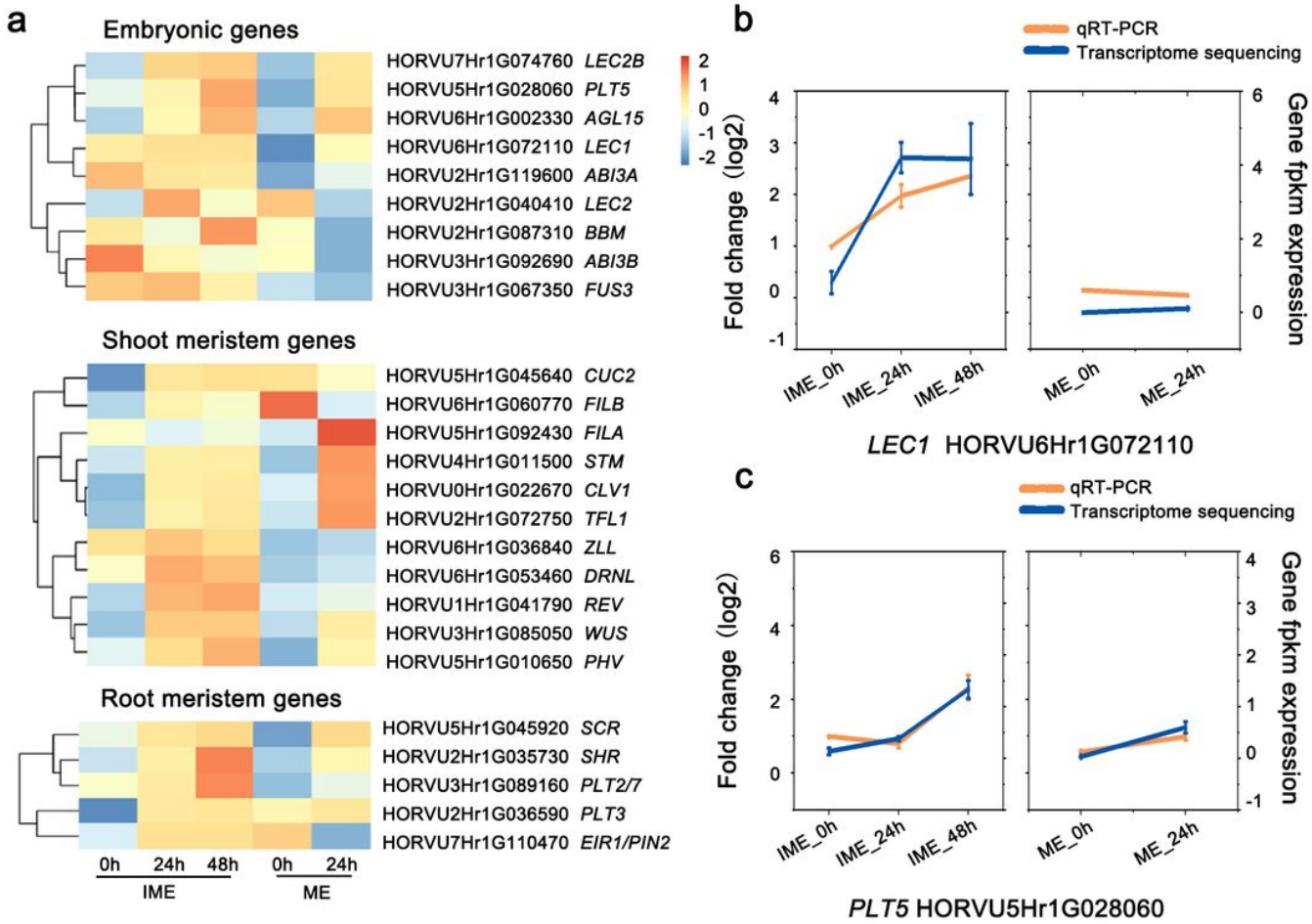

Figure 5

Heatmap showing expression changes of key developmental genes for embryos and meristems during callus induction. The expression levels were visualized by using OmicStudio tools at https://www.omicstudio.cn/tool based on RNA-seq datasets (Additional file 2: Supplementary raw data). a: Clustering display of expression intensities of the embryonic, shoot, and root meristem genes based on RNA-seq datasets. b: The transcript levels of LEC1 and PLT5 in five samples were revealed by qRT-PCR and RNA-seq data. The data shown are means ± S.D. of three biological replicates.

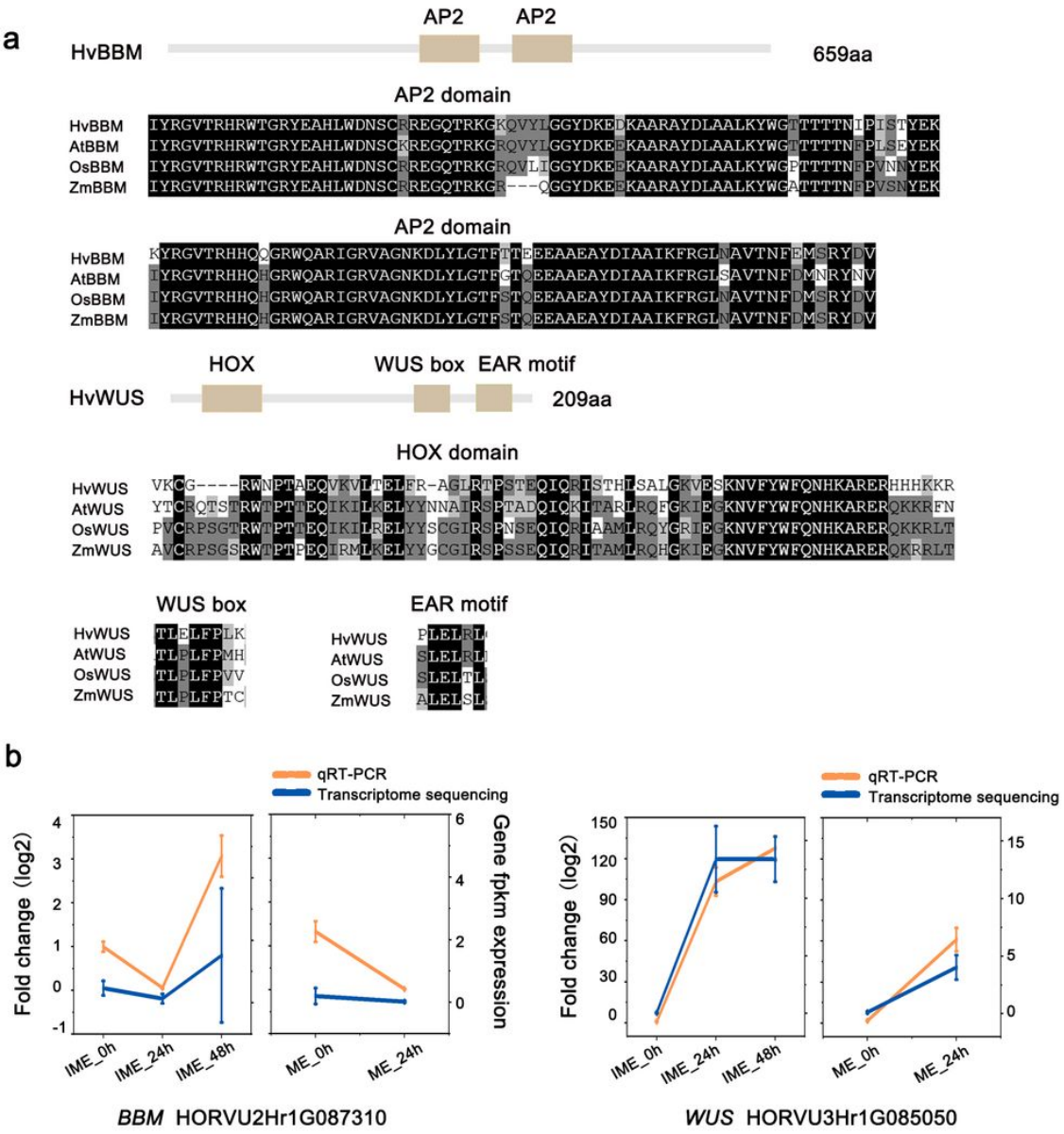

Figure 6

Identification of BBM and WUS candidate genes in barley and its expression response to callus-inducing medium (CIM). a: Sequence alignment and domain analysis of the BBM and WUS in Arabidopsis, rice, maize, and barley. b: The transcript levels of BBM and WUS in the five samples were revealed by qRT-PCR and RNA-seq data. The data shown are means ± S.D. of three biological replicates.

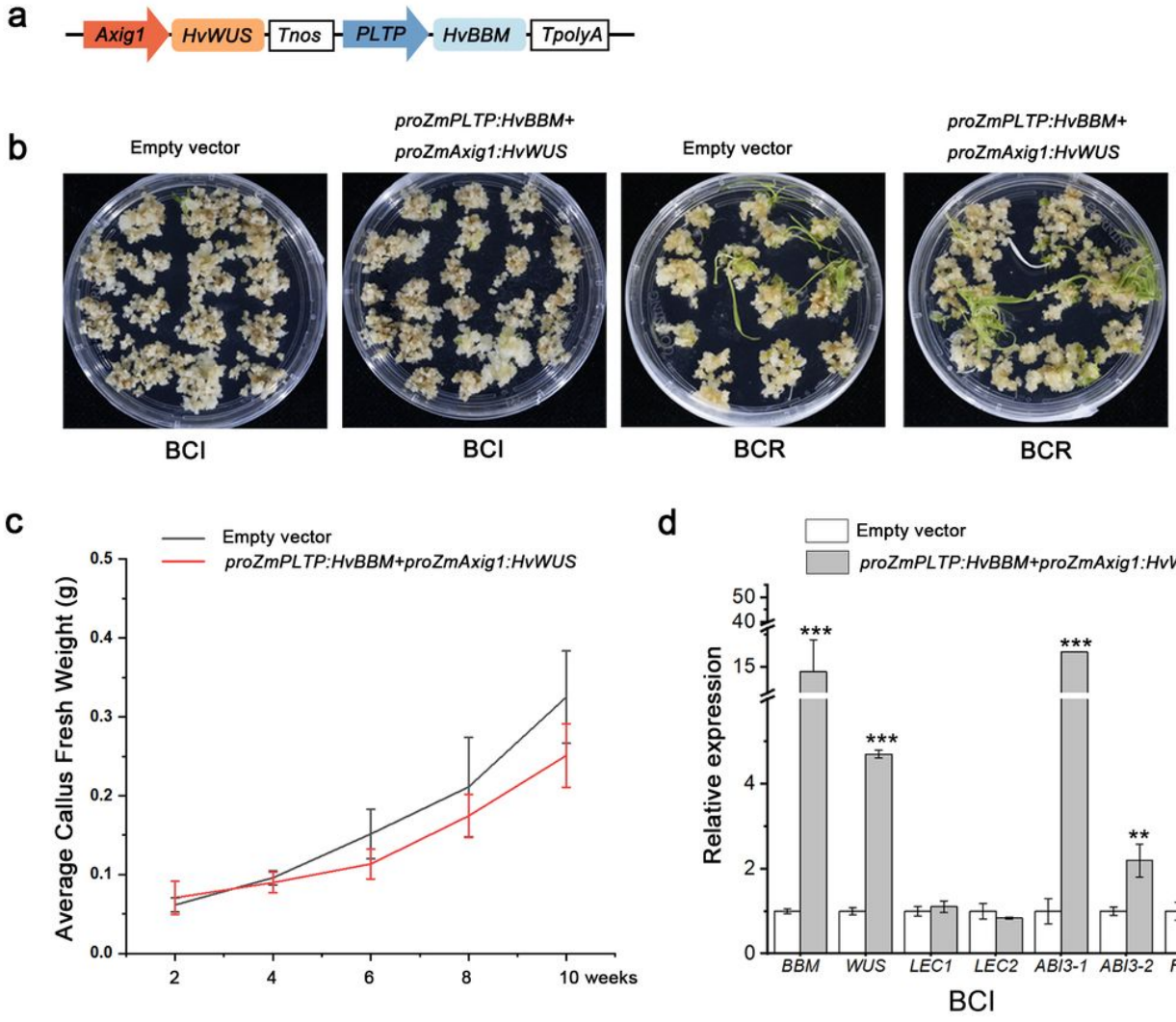

Figure 7

The effect of BBM and WUS ectopic expression on callus-inducing medium (CIM)-induced callus formation and transformation efficiency. a: Schematic representation of the construct used for Agrobacterium-mediated barley transformation. The proZmPLTP:HvBBM+proZmAxig1:HvWUS construct contained two cassettes: the first one included the maize phospholipid transferase promoter (proZmPLTP) driving HvBBM with a Nos terminator, and the second one included the maize Axig1 promoter (proZmAxig1) driving HvWUS with a Nos terminator. b: The callus-forming and plant regeneration phenotype after Agrobacterium inoculation. The group using an empty vector was set as control. c: Fresh weight analysis of callus in control and proZmPLTP:HvBBM+proZmAxig1:HvWUS transformation group. Error bars indicate the SE of the mean (n=30); **, $P < 0.01$ (Student's t-test). The experiments were performed in three independent replicates. d: The effect of BBM and WUS ectopic expression on the genes in the LEC1-ABI3-FUS3-LEC2 network. The data shown are means ± S.D. of three biological replicates.

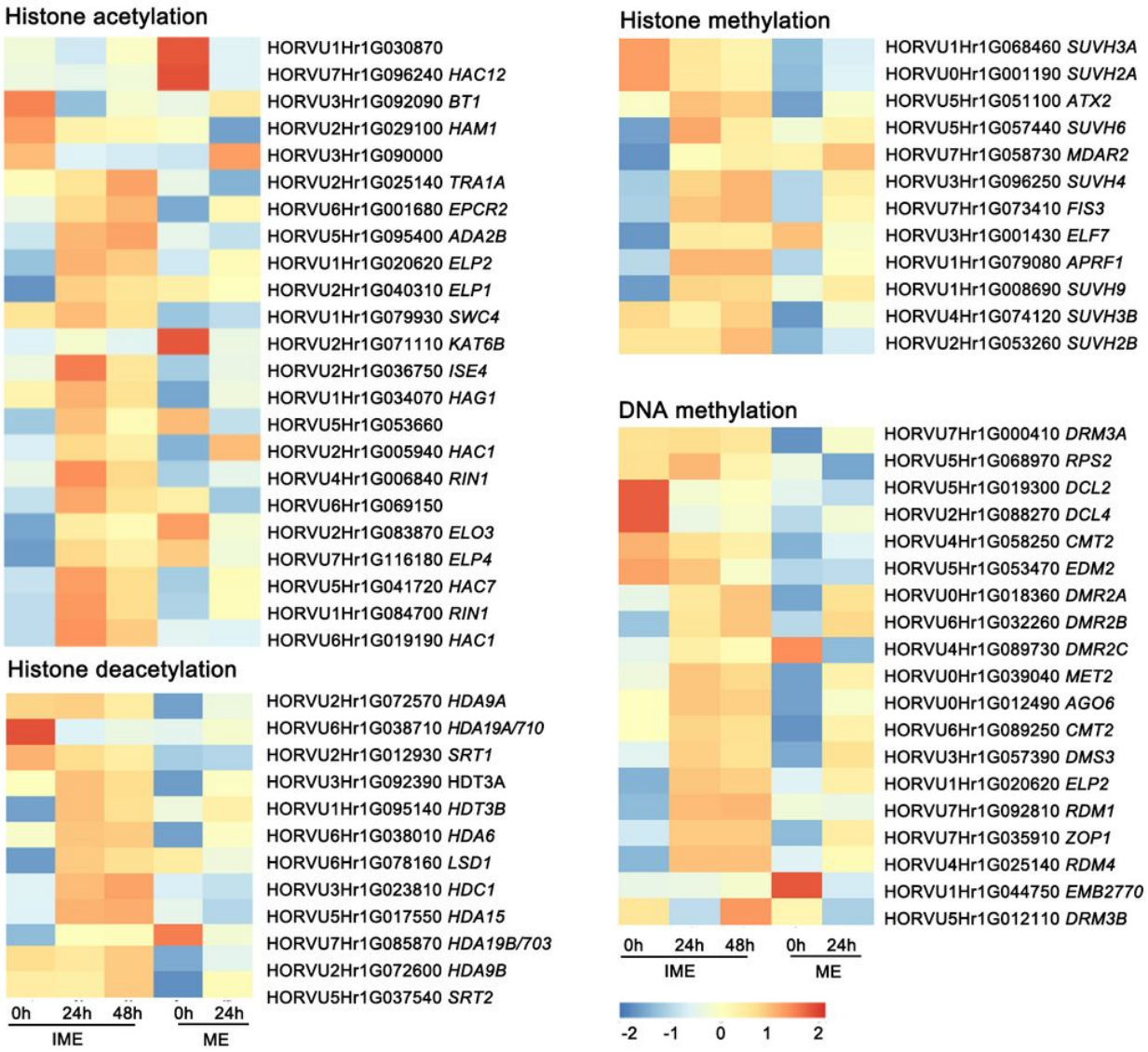

Figure 8

Transcriptional changes of genes regulating DNA methylation and histone modification. The expression levels were visualized by using OmicStudio tools at https://www.omicstudio.cn/tool based on RNA-seq datasets (Additional file 2: Supplementary raw data). Numbers beneath the heat map indicate the relative expression intensities, and the higher expression intensities are indicated by more reddish colors. Note that only genes with RPKM>1 are shown.

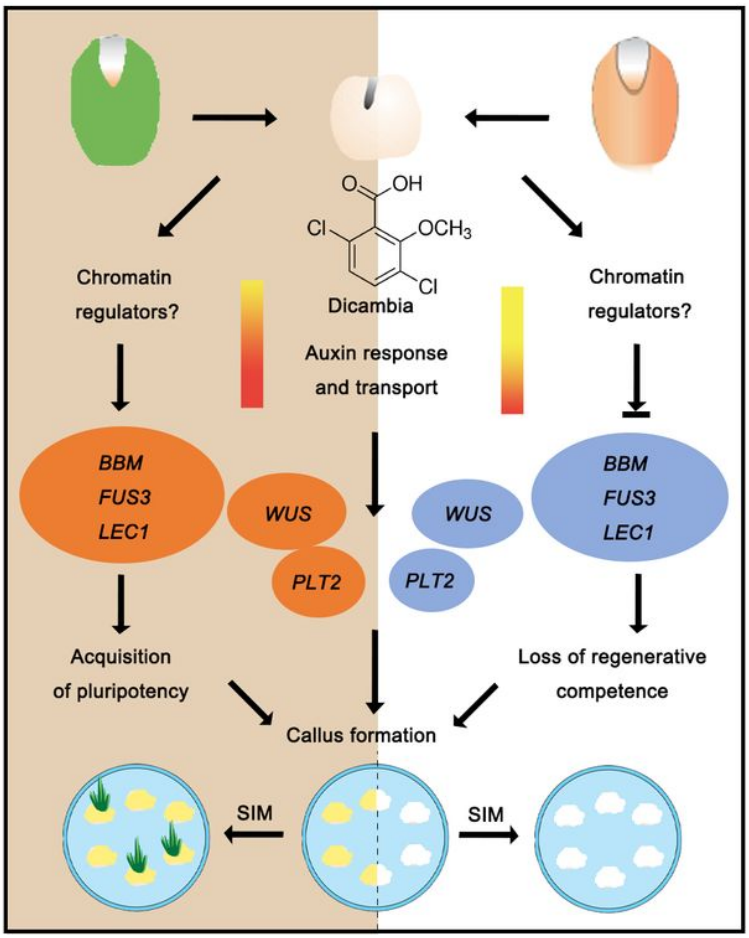

Figure 9

A schematic diagram describing gene expression regulation during immature and mature barley embryo-derived callus formation. Dicamba (synthetic auxin) induces cell fate transition through the auxin signaling pathway, and more genes are included in the IME system (left) than in the IM system (right). Embryonic genes BBM, LEC1, and FUS3, shoot meristem gene WUS, and root meristem gene PLT2 displayed differential expression patterns between the two systems, resulted in the production of different types of callus. Embryonic callus (left) and nonembryonic callus (right) exhibit differential regeneration potential on shoot inducing medium (SIM). Orange color presents significantly up-regulated genes, while blue color presents genes which were activated slightly or remain unchanged. Epigenetic modification might be involved in regulating the expression status of regulatory genes in different explants and their responses to callus induction.

Supplementary Files

This is a list of supplementary files associated with this preprint. Click to download.

- Addintionfile1.pdf
- Addintionfile2SupplementaryRawdata.xlsx